

## UNSTEADY TWO-LAYERED FLUID FLOW AND HEAT TRANSFER OF CONDUCTING FLUIDS IN A CHANNEL BETWEEN PARALLEL POROUS PLATES UNDER TRANSVERSE MAGNETIC FIELD

T. LINGA RAJU\* and M. NAGAVALLI  
 Department of Engineering Mathematics  
 Andhra University College of Engineering (A)  
 Visakhapatnam, Pin code: 530 003, INDIA  
 E-mail: tlraju45@yahoo.com

The unsteady magnetohydrodynamic flow of two immiscible fluids in a horizontal channel bounded by two parallel porous isothermal plates in the presence of an applied magnetic and electric field is investigated. The flow is driven by a constant uniform pressure gradient in the channel bounded by two parallel insulating plates, one being stationary and the other oscillating, when both fluids are considered as electrically conducting. Also, both fluids are assumed to be incompressible with variable properties, viz. different viscosities, thermal and electrical conductivities. The transport properties of the two fluids are taken to be constant and the bounding plates are maintained at constant and equal temperatures. The governing equations are partial in nature, which are then reduced to the ordinary linear differential equations using two-term series. Closed form solutions for velocity and temperature distributions are obtained in both fluid regions of the channel. Profiles of these solutions are plotted to discuss the effect on the flow and heat transfer characteristics, and their dependence on the governing parameters involved, such as the Hartmann number, porous parameter, ratios of the viscosities, heights, electrical and thermal conductivities.

**Key words:** magnetohydrodynamics, two-layered fluid flow/immiscible fluids, unsteady flow, oscillatory motion, heat transfer, porous plates.

### 1. Introduction

Many problems relating to plasma physics, aeronautics, geophysics and in petroleum industry, also in industrial applications, etc; involve multi layered-fluid flow situations. In the petroleum industry as well as in other engineering and technological fields, a stratified two-phase/two-layered fluid flow often occurs. For example, in geophysics, it is so important to study the interaction of the geomagnetic field with the hot springs/fluids in geothermal regions, in which, once the interaction of the geomagnetic field with the flow field is known, then one can easily find the temperature distribution from the well known energy equation. Moreover, the temperature distribution plays an important role in MHD generators, plasma physics, turbines, etc. Also it is a known fact that, to generate electricity, the temperature is used to run the turbine across a magnetic field. Further, recent studies show that magnetohydrodynamic (MHD) flows can also be a viable option for transporting conducting fluids in microscale systems, such as the flow inside micro-channel networks of a lab-on-a-chip device (Haim *et al.*, 2003; Hussameddine *et al.*, 2008). In micro-fluidic devices, multiple fluids can be transported through a channel for different reasons. For example, an increase in mobility of a fluid may be achieved by stratification of a highly mobile fluid or mixing of two or more fluids in transit may be designed for emulsification or heat and mass transfer applications. In this regard, magnetic field-driven micro-pumps are an increasing demand due to their long-term reliability in generating flow, low power requirement and mixing efficiency (Qian *et al.*, 2002; Weston *et al.*, 2010).

---

\* To whom correspondence should be addressed

The unsteady magnetohydrodynamic flow and heat transfer, due to the imposed oscillations/impulsive motion of a boundary or boundary temperature under the presence of an external magnetic field has received much attention. The problem of magnetohydrodynamic effects on the unsteady Couette flow was investigated by Tao (1960), Katagiri (1962) and many others. Muhuri (1963) considered the flow formation in Couette motion of an electrically conducting fluid subject to a magnetic field under different conditions. Gupta (1960) studied the magnetohydrodynamic flow near an accelerated plate. This problem was extended by Soundalgekar (1967) with taking another parallel plate at a finite distance from the accelerated plate. Stanisic *et al.* (1962) extended Schlichting's (1955) problem to the case of a hydromagnetic fluid flow between two oscillating flat plates. Varma and Gaur (1972) investigated an unsteady flow and temperature distribution of a viscous incompressible fluid flow between two parallel flat plates. Pallath Chandran *et al.* (1998) discussed an unsteady hydromagnetic free convection flow with heat flux and accelerated boundary motion. Raju and Murty (2005) studied quasi-steady state solutions of an unsteady ionized hydromagnetic flow and heat transfer between two parallel walls in a rotating system.

All the above mentioned studies are related to single-fluid flow configurations. But most of the problems related to the petroleum industry, geophysical fluid dynamics, plasma physics, magnetohydrodynamics and many such areas involve multi-layered-fluid flow situations. Transportation and extraction of the products of oil are other obvious applications using a two-phase system to obtain the increased flow rates in an electromagnetic pump from the possibility of reducing the power required to pump oil in a pipe line by a suitable addition of water (Shail, 1973). There are several investigations with regards to both experimental and theoretical aspects of magnetohydrodynamic two-phase/two-layered fluids flow problems, which are available in the literature during the last few decades [viz., Lielausis, 1975; Michiyoshi *et al.*, 1977; Chan, 1979; Chao *et al.*, 1979; Dunn, 1980; Gherson, 1984; Lohrasbi and Sahai, 1989; Serizawa *et al.*, 1990; Malashetty and Leela, 1992; Ramadan and Chamkha, 1999; Raju and Murty, 2006; Tsuyoshi Inoue and Shu-Ichiro Inutsuka, 2008; etc]. But research studies corresponding to the unsteady fluid flow problems are limited in number. Moreover, a significant number of practical problems dealing with immiscible fluids are unsteady in nature. Also, in many practical problems, it is advantageous to consider both immiscible fluids as electrically conducting, one of which is highly electrically conducting compared to the other. The fluid of low electrical conductivity compared to the other is helpful to reduce the power required to pump the fluid in MHD pumps and flow meters. In view of these; Chamkha (2004) studied the unsteady MHD convective heat and mass transfer past a semi-infinite vertical permeable moving plate with heat absorption. Umavathi *et al.* (2006) investigated the oscillatory Hartmann two-fluid flow and heat transfer in a horizontal channel. Raju and Sreedhar (2009) discussed an unsteady two-fluid flow and heat transfer of conducting fluids in channels under a transverse magnetic field.

So, keeping in view the wide area of practical importance of multi-layered fluid flows as mentioned above, it is the objective of the present study to investigate the behaviour of flow formation and heat transfer aspects of an unsteady MHD two-fluid flow of electrically conducting fluids in a horizontal channel bounded by two parallel porous plates under the influence of a transversely applied uniform strong magnetic field. The flow is driven by a constant uniform pressure gradient in a channel bounded by two parallel porous plates, one being stationary and the other oscillating. The two fluids are assumed to be incompressible and electrically conducting with different viscosities, thermal and electrical conductivities. The transport properties of the two fluids are considered as constant and the bounding plates, (which are infinite in extent) are maintained at constant and equal temperatures. The governing partial differential equations are reduced to the ordinary linear differential equations using two-term series. These equations are solved analytically to obtain exact solutions for the velocity distributions, such as,  $u_1$ , and  $u_2$  in the two regions, respectively, by assuming that their solutions are a combination of both the steady state and time dependent components of the solutions. Closed form solutions for temperature distributions, namely,  $\theta_1$  and  $\theta_2$  in the two regions are determined by using the solutions of velocity distributions obtained already. Numerical values of the velocity and temperature distributions are computed for different sets of values of the governing parameters involved in the study and their corresponding profiles are also plotted to illustrate the details of the flow and heat transfer characteristics and their dependence on the governing parameters, such as the Hartmann number, porous parameter, viscosity ratio, electrical and thermal conductivities, height ratio. Also an observation is

made how the velocity and temperature distributions vary with the hydromagnetic interaction in the case of steady and unsteady flow motions.

Moreover, the results of this study are expected to be useful in understanding the effect of the presence of a slag layer on heat transfer characteristics of a coal fired MHD generator, flow meters, in nuclear reactor technology and in space crafts, etc. Also, such flows are encountered in many industrial applications, such as liquid metals, metal working process, geothermal energy extracts and many other applications. It is also important to understand the dynamics of interfaces between the fluids and its effect on the transport characteristics of the system.

This paper is arranged as follows. In § 1, introduction of the problem is given. The equations of motion, energy, the boundary and interface conditions are given in § 2. Closed form solutions of the problem are given in § 3, while § 4 gives the results and discussion based on the velocity and temperature profiles, which are shown in Figs 2 to 12.

## 2. Mathematical formulation of the governing equations of motion, energy, boundary and interface conditions

Consider an unsteady hydromagnetic two layered-fluid flow in a horizontal channel consisting of two infinite parallel plates extending along the  $x$ - and  $z$ -directions defined by the planes  $y = h_1$  and  $y = -h_2$ , as shown in Fig.1, which represents the physical configuration and flow model choosing the origin midway between the two plates. The flow in both upper and lower regions is driven by a common constant pressure gradient  $\left(-\frac{\partial p}{\partial x}\right)$ .

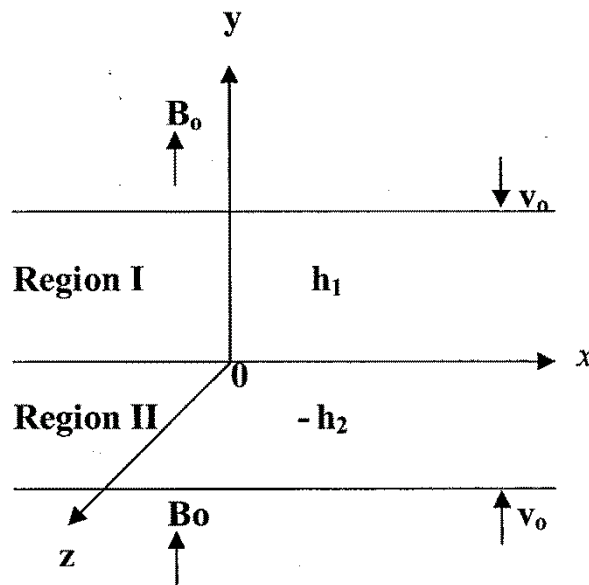


Fig.1. Physical configuration and flow model.

The fluid is subjected to a constant section  $v_0$  applied normal to both the plates and hence if  $(u_i, v_i, w_i), (i = 1, 2)$ , are the velocity components in the two fluids, then the equation of continuity  $\nabla \cdot \bar{q}_i = 0$  gives  $v_i = -v_0 (v_0 > 0)$  where  $\bar{q}_i = (u_i, v_i, w_i)$ . The regions  $0 \leq y \leq h_1$  and  $-h_2 \leq y \leq 0$  are occupied by two immiscible electrically conducting, incompressible fluids with different viscosities  $\mu_1, \mu_2$ , thermal conductivities  $K_1, K_2$  and electrical conductivities  $\sigma_1, \sigma_2$ . A constant magnetic field of strength  $B_0$  is

applied transverse to the flow direction, that is along the  $y$ -direction. Also, a constant electric field  $E_0$  is applied in the  $z$ -direction. The induced magnetic field is neglected by assuming that it is small when compared with the applied field. The two bounding plates are maintained at a constant temperature  $T_w$ . With these assumptions, the non-dimensional governing equations of motion, current and energy and the corresponding boundary and interface conditions (as in Lohrasbi and Shahai 1989; Malashetty and Leela 1992 and Raju and Murty, 2005) for both fluid regions are expressed as

### Region-I

$$\rho_1 \frac{\partial u_1}{\partial t} - \mu_1 \frac{\partial^2 u_1}{\partial y^2} + \rho_1 v_0 \frac{\partial u_1}{\partial y} + \frac{\partial p}{\partial x} + \sigma_1 u_1 B_0^2 + \sigma_1 E_0 B_0 = 0, \quad (2.1)$$

$$\rho_1 c_{p1} \frac{\partial T_1}{\partial t} - K_1 \frac{\partial^2 T_1}{\partial y^2} + \rho_1 v_0 \frac{\partial T_1}{\partial y} - \mu_1 \left( \frac{\partial u_1}{\partial y} \right)^2 - \sigma_1 u_1^2 B_0^2 - \sigma_1 E_0^2 - 2\sigma_1 u_1 B_0 E_0 = 0. \quad (2.2)$$

### Region II

$$\rho_2 \frac{\partial u_2}{\partial t} - \mu_2 \frac{\partial^2 u_2}{\partial y^2} + \rho_2 v_0 \frac{\partial u_2}{\partial y} + \frac{\partial p}{\partial x} + \sigma_2 u_2 B_0^2 + \sigma_2 B_0 E_0 = 0, \quad (2.3)$$

$$\rho_2 c_{p2} \frac{\partial T_2}{\partial t} - K_2 \frac{\partial^2 T_2}{\partial y^2} + \rho_2 v_0 \frac{\partial T_2}{\partial y} - \mu_2 \left( \frac{\partial u_2}{\partial y} \right)^2 - \sigma_2 u_2^2 B_0^2 - \sigma_2 E_0^2 - 2\sigma_2 u_2 B_0 E_0 = 0. \quad (2.4)$$

Here subscripts 1 and 2 represent the values for Region-I and Region-II, respectively, where  $u_1, u_2$  are the  $x$ -component of fluid velocities;  $T_1, T_2$  are the fluid temperatures in the two regions, respectively, and ' $t$ ' is the time. The boundary conditions on velocity are the no-slip boundary condition at the lower plate and an oscillatory one at the upper plate. The boundary conditions on temperature are isothermal conditions. We also assume the continuity of velocity, shear stress, temperature and heat flux at the interface between the two fluid layers at  $y = 0$ .

The boundary and interface conditions for the two fluids are considered as

$$u_1(h_1) = 0, \quad \text{for } t \leq 0, \quad (2.5)$$

$$= \text{Real}(\varepsilon e^{i\omega t}), \quad \text{for } t > 0.$$

$$u_2(h_2) = 0, \quad (2.6)$$

$$u_1(0) = u_2(0), \quad (2.7)$$

$$\mu_1 \frac{du_1}{dy} = \mu_2 \frac{du_2}{dy} \quad \text{at } y = 0 \quad (2.8)$$

where  $\varepsilon$  (amplitude) is a small constant quantity such that  $\varepsilon \ll l$  and  $\omega$  is the frequency of oscillation at the plate, and the perturbed fields initially are zero, because the system is at rest for  $t \leq 0$ .

Since the walls are maintained at the same temperature, the boundary and interface conditions on temperature for both the fluids are given by

$$T_1(h_1) = T_w, \quad (2.9)$$

$$T_2(-h_2) = T_w, \quad (2.10)$$

$$T_1(0) = T_2(0), \quad (2.11)$$

$$K_1 \frac{dT_1}{dy} = K_2 \frac{dT_2}{dy} \quad \text{at} \quad y = 0. \quad (2.12)$$

The above Eqs (2.1)-(2.4) are non-dimensionalised using the following dimensionless quantities

$$u^*_1 = \frac{u_1}{u_p}, \quad u^*_2 = \frac{u_2}{u_p}, \quad y^*_i = \left( \frac{y_i}{h_i} \right) (i = 1, 2), \quad u_p = \left( \frac{\partial p}{\partial x} \right) \frac{h_1^2}{\mu_1}, \quad t^* = \frac{\nu_1 t}{h_1^2}, \quad \omega^* = \frac{\omega h_1^2 \rho_1}{\mu_1},$$

$$M^2 \text{ (Hartmann number)} = B_0^2 h_1^2 \left( \frac{\sigma_1}{\mu_1} \right), \quad \lambda \text{ (porous parameter)} = \frac{h_1 \rho_1 \nu_0}{\mu_1},$$

$$\alpha \text{ (ratio of the viscosities)} = \frac{\mu_1}{\mu_2}, \quad h \text{ (ratio of the heights)} = \frac{h_2}{h_1},$$

$$\sigma \text{ (ratio of the electrical conductivities)} = \frac{\sigma_1}{\sigma_2}, \quad \beta \text{ (ratio of thermal conductivities)} = \frac{K_1}{K_2},$$

$$\theta_i = \frac{T_i - T_w}{\mu_p^2 \mu_2 / K_i}, \quad R_e \text{ (electric load parameter)} = E_0 / B_0 u_p. \quad (2.13)$$

With the use of these transformations and Eq.(2.13) and for simplicity neglecting the asterisks, the non-dimensional forms of Eqs (2.1) to (2.4) for both the fluid regions are written as

### Region-I

$$\frac{du_1}{dt} - \frac{d^2 u_1}{dy^2} + \lambda \frac{du_1}{dy} + M^2 (R_e + u_1) - 1 = 0, \quad (2.14)$$

$$\frac{d\theta_1}{dt} - \frac{d^2 \theta_1}{dy^2} + \lambda \frac{d\theta_1}{dy} - \left( \frac{du_1}{dy} \right)^2 - M^2 (R_e + u_1)^2 = 0. \quad (2.15)$$

### Region-II

$$\frac{du_2}{dt} - \frac{d^2 u_2}{dy^2} + \lambda \frac{du_2}{dy} + M^2 h^2 \alpha \sigma (R_e + u_2) - \alpha h^2 = 0, \quad (2.16)$$

$$\frac{d\theta_2}{dt} - \frac{d^2\theta_2}{dy^2} + \lambda \frac{d\theta_2}{dy} - \frac{\beta}{\alpha} \left( \frac{du_2}{dy} \right)^2 - M^2 h^2 \beta \sigma (R_e + u_2) = 0. \quad (2.17)$$

The non-dimensional forms of the velocity, temperature and interface boundary conditions become

$$\begin{aligned} u_1(+1) &= 0, & \text{for } t &\leq 0, \\ &= Re(\varepsilon e^{i\omega t}), & \text{for } t &> 0. \end{aligned} \quad (2.18)$$

$$u_2(-1) = 0, \quad (2.19)$$

$$u_1(0) = u_2(0), \quad (2.20)$$

$$\frac{du_1}{dy} = (1/\alpha h) \frac{du_2}{dy} \quad \text{at } y = 0, \quad (2.21)$$

$$\theta_1(+1) = 0, \quad (2.22)$$

$$\theta_2(-1) = 0, \quad (2.23)$$

$$\theta_1(0) = \theta_2(0), \quad (2.24)$$

$$\frac{d\theta_1}{dy} = (1/\beta h) (d\theta_2/dy) \quad \text{at } y = 0. \quad (2.25)$$

Condition (2.19) represents the no-slip condition at the lower wall and the condition (2.18) is due to oscillation of the upper wall. Conditions (2.20) and (2.21) represent the continuity of velocity and shear stress at the interface  $y = 0$ . The conditions (2.22) and (2.23) represent the isothermal conditions, while the conditions (2.24) and (2.25) represent the continuity of temperature and heat flux at the interface  $y = 0$ .

### 3. Solutions of the problem

The governing momentum Eqs (2.14) and (2.16) along with the energy Eqs (2.15) and (2.17) are to be solved subject to the boundary and interface conditions (2.18) and (2.25) for the velocity and temperature distributions in both regions. These equations are coupled partial differential equations that cannot be solved in a closed form. But they can be reduced to ordinary linear differential equations by assuming the following two term series

$$u_1(y, t) = u_{01}(y) + (\varepsilon \cos \omega t) u_{11}(y), \quad (3.1)$$

$$u_2(y, t) = u_{02}(y) + (\varepsilon \cos \omega t) u_{12}(y), \quad (3.2)$$

$$\theta_1(y, t) = \theta_{01}(y) + (\varepsilon \cos \omega t) \theta_{11}(y), \quad (3.3)$$

$$\theta_2(y, t) = \theta_{02}(y) + (\varepsilon \cos \omega t) \theta_{12}(y), \quad (3.4)$$

here, the terms  $u_{01}(y), u_{02}(y)$  and  $\theta_{01}(y), \theta_{02}(y)$  are velocity and temperature distribution in the basic steady state case in two regions, while,  $u_{11}(y), u_{12}(y)$  and  $\theta_{11}(y), \theta_{12}(y)$  are the corresponding time dependent components of the solutions, which are the factors of  $\text{Real}(\varepsilon e^{i\omega t})$  to be determined with the help of Eqs (2.14) to (2.17).

By substituting the expressions (3.1)-(3.4) into Eqs (2.14)-(2.17) and separating the steady state and transient time varying components, the following differential equations for  $u_{01}(y), u_{02}(y)$  and  $\theta_{01}(y), \theta_{02}(y)$ ; also,  $u_{11}(y), u_{12}(y)$  and  $\theta_{11}(y), \theta_{12}(y)$  in pairs are obtained in both regions as

### Region-I

#### For the steady-state part

$$\frac{d^2 u_{01}}{dy^2} - \lambda \frac{du_{01}}{dy} - a_1 u_{01} = a_2, \quad (3.5)$$

$$\frac{d^2 \theta_{01}}{dy^2} - \lambda \frac{d\theta_{01}}{dy} = -b_{14} e^{2m_1 y} - b_{15} e^{2m_2 y} - b_{16} e^{m_1 y} - b_{17} e^{m_2 y} - b_{18} e^{b_4 y} + b_{19}. \quad (3.6)$$

#### For the transient time dependent part

$$\frac{d^2 u_{11}}{dy^2} - a_6 \frac{du_{11}}{dy} - a_7 u_{11} = 0, \quad (3.7)$$

$$\frac{d^2 \theta_{11}}{dy^2} - \lambda \frac{d\theta_{11}}{dy} + b_{68} \theta_{11} = -b_{78} e^{2m_5 y} - b_{79} e^{2m_6 y} - b_{76} e^{m_5 y} - b_{77} e^{m_6 y} - b_{80} e^{b_{72} y}. \quad (3.8)$$

### Region-II

#### For the steady-state part

$$\frac{d^2 u_{02}}{dy^2} - \lambda \frac{du_{02}}{dy} - a_8 u_{02} = a_9, \quad (3.9)$$

$$\frac{d^2 \theta_{02}}{dy^2} - \lambda \frac{d\theta_{02}}{dy} = -b_{35} e^{2m_3 y} - b_{36} e^{2m_4 y} - b_{37} e^{m_3 y} - b_{38} e^{m_4 y} - b_{39} e^{b_{25} y} + b_{40}. \quad (3.10)$$

#### For the transient time dependent part

$$\frac{d^2 u_{12}}{dy^2} - a_{12} \frac{du_{12}}{dy} - a_{13} u_{12} = 0, \quad (3.11)$$

$$\frac{d^2\theta_{12}}{dy^2} - \lambda \frac{d\theta_{12}}{dy} + b_{68}\theta_{12} = -b_{103}e^{2m_7y} - b_{104}e^{2m_8y} - b_{101}e^{m_7y} - b_{102}e^{m_8y} - b_{105}e^{b_{97}y}. \quad (3.12)$$

The corresponding boundary and interface conditions on velocity and temperature become:

**For the steady-state part**

$$u_{01}(+1) = 0, \quad u_{02}(-1) = 0, \quad u_{01}(0) = u_{02}(0), \quad (3.13)$$

$$\frac{du_{01}}{dy} = \frac{1}{\alpha h} \frac{du_{02}}{dy} \quad \text{at} \quad y = 0. \quad (3.14)$$

$$\theta_{01}(+1) = 0, \quad \theta_{02}(-1) = 0, \quad \theta_{01}(0) = \theta_{02}(0), \quad (3.15)$$

$$\frac{d\theta_{01}}{dy} = \frac{1}{\beta h} \frac{d\theta_{02}}{dy} \quad \text{at} \quad y = 0. \quad (3.16)$$

**For the transient time dependent part**

$$u_{11}(+1) = 1, \quad u_{12}(-1) = 0, \quad u_{11}(0) = u_{12}(0), \quad (3.17)$$

$$\frac{du_{11}}{dy} = \frac{1}{\alpha h} \frac{du_{12}}{dy} \quad \text{at} \quad y = 0, \quad (3.18)$$

$$\theta_{11}(+1) = 0, \quad \theta_{12}(-1) = 0, \quad \theta_{11}(0) = \theta_{12}(0), \quad (3.19)$$

$$\frac{d\theta_{11}}{dy} = \frac{1}{\beta h} \frac{d\theta_{12}}{dy} \quad \text{at} \quad y = 0. \quad (3.20)$$

The above Eqs (3.5) to (3.12) along with the boundary and interface conditions (3.13) to (3.20) represent a system of ordinary linear differential equations and conditions, these can be solved in a closed form separately in two parts. Hence, the final solutions for velocity and temperature distributions of the unsteady flow problem are obtained as:

**Region-I**

$$u_1(y,t) = c_1 e^{m_1 y} + c_2 e^{m_2 y} - \frac{a_2}{a_1} + R_e \left( \varepsilon e^{i\omega t} \right) \left( c_5 e^{m_5 y} + c_6 e^{m_6 y} \right), \quad (3.21)$$

$$\theta_1(y,t) = d_1 + d_2 e^{\lambda \cdot y} + b_{41} e^{2m_1 y} + b_{42} e^{2m_2 y} + b_{43} e^{m_1 y} + b_{44} e^{m_2 y} + b_{45} e^{b_4 y} + b_{46} y + R_e \left( \varepsilon e^{i\omega t} \right) \left( d_5 e^{m_9 y} + d_6 e^{m_{10} y} + b_{81} e^{2m_5 y} + b_{82} e^{2m_6 y} + b_{83} e^{m_5 y} + b_{84} e^{m_6 y} + b_{85} e^{b_{72} y} \right). \quad (3.22)$$



**Region-II**

$$u_2(y,t) = c_3 e^{m_3 y} + c_4 e^{m_4 y} - \frac{a_9}{a_8} + R_e \left( \varepsilon e^{i\omega t} \right) \left( c_7 e^{m_7 y} + c_8 e^{m_8 y} \right), \quad (3.23)$$

$$\begin{aligned} \theta_2(y,t) = & d_3 + d_4 e^{\lambda \cdot y} + b_{47} e^{2m_3 y} + b_{48} e^{2m_4 y} + b_{49} e^{m_3 y} + b_{50} e^{m_4 y} + b_{51} e^{b_{25} y} \\ & + b_{52} y + R_e \left( \varepsilon e^{i\omega t} \right) \left( d_7 e^{m_{11} y} + d_8 e^{m_{12} y} + b_{106} e^{2m_7 y} + b_{107} e^{2m_8 y} + b_{108} e^{m_7 y} + \right. \\ & \left. + b_{109} e^{m_8 y} + b_{110} e^{b_{97} y} \right). \end{aligned} \quad (3.24)$$

The solutions of the non-periodic terms represent the steady-state flow solutions for both fluid regions, without going into detail, the steady-state velocity and temperature profiles are shown in Figs 2 to 12. The solution of the periodic terms gives the transient velocity and temperature distribution in both regions of the channel. The solutions for the unsteady problem given by Eqs (3.21)-(3.24) are evaluated numerically for different non-dimensional governing flow parameters and these results are plotted, in Figs 2 to 12. Here the value for  $\varepsilon$  is fixed at 0.5 for all graphs.

The constants appearing in the above solutions are given in the Appendix.

**1.4. Results and discussion**

The problem of an unsteady MHD two immiscible fluid flow and heat transfer through a horizontal channel bounded by two parallel porous plates is investigated analytically in the presence of an applied transverse magnetic field. The two fluids are assumed to be incompressible and electrically conducting with different viscosities, thermal and electrical conductivities. The resulting partial differential equations are reduced to ordinary linear differential equations and solved analytically by means of the assumed solutions using two-term series. Exact solutions for the velocity distributions, such as,  $u_1$ ,  $u_2$  respectively in the two regions are obtained. Then the closed form solutions for temperature distributions, namely,  $\theta_1$  and  $\theta_2$  in the two regions are determined by making use of the already obtained solutions of velocity distributions. The profiles for the velocity and temperature distributions for both steady state and unsteady state flow are shown in Figs 2 to 12 and the important features of hydromagnetic and thermal state of the fluids in the two regions by varying one of the governing parameters, while the others are held fixed are discussed. The solid lines show the profiles for an unsteady motion and the dash-dot lines show the steady flow.

The effect of varying the Hartmann number  $M$  on velocity and temperature distributions is shown in Figs 2 and 3. It can be seen that the effect of increasing  $M$  increases the velocity distributions  $u_1$ ,  $u_2$  and temperature distribution  $\theta_1$ ,  $\theta_2$  in the two fluid regions. This implies that the velocity of the fluid increases as the strength of the magnetic field increases, which means the body force is an accelerating force. Due to this accelerating force the fluid temperatures are actually increased and hence, at the commencement of motion this tendency is significant. Also, the maximum velocity in the channel tends to move above the channel centre line towards region-I (i.e., in the upper fluid region) as the Hartmann number  $M$  increases, when all the remaining governing parameters are fixed.

Figures 4 and 5 show the effect of the porous parameter  $\lambda$  on both velocity and temperature distributions in the fluid regions. From Fig.4 it is noted that the velocity distributions in the two regions increase as  $\lambda$  increases. The maximum velocity distribution in the channel tends to move above the channel center line towards region-I as  $\lambda$  increases. While from Fig.5, it is seen that the temperature increases in the upper region and decreases in the lower as  $\lambda$  increases.

The effect of varying the electrical conductivity ratio  $\sigma$  on the velocity and temperature distribution is shown in Figs 6 and 7. It is noted that both velocity and temperature distributions as well as  $\sigma$  increase. The maximum velocity distribution in the channel tends to move above the channel centre line towards region-I as  $\sigma$  increases, while the temperature distribution in the channel tends to move below the channel centre line towards region-II.

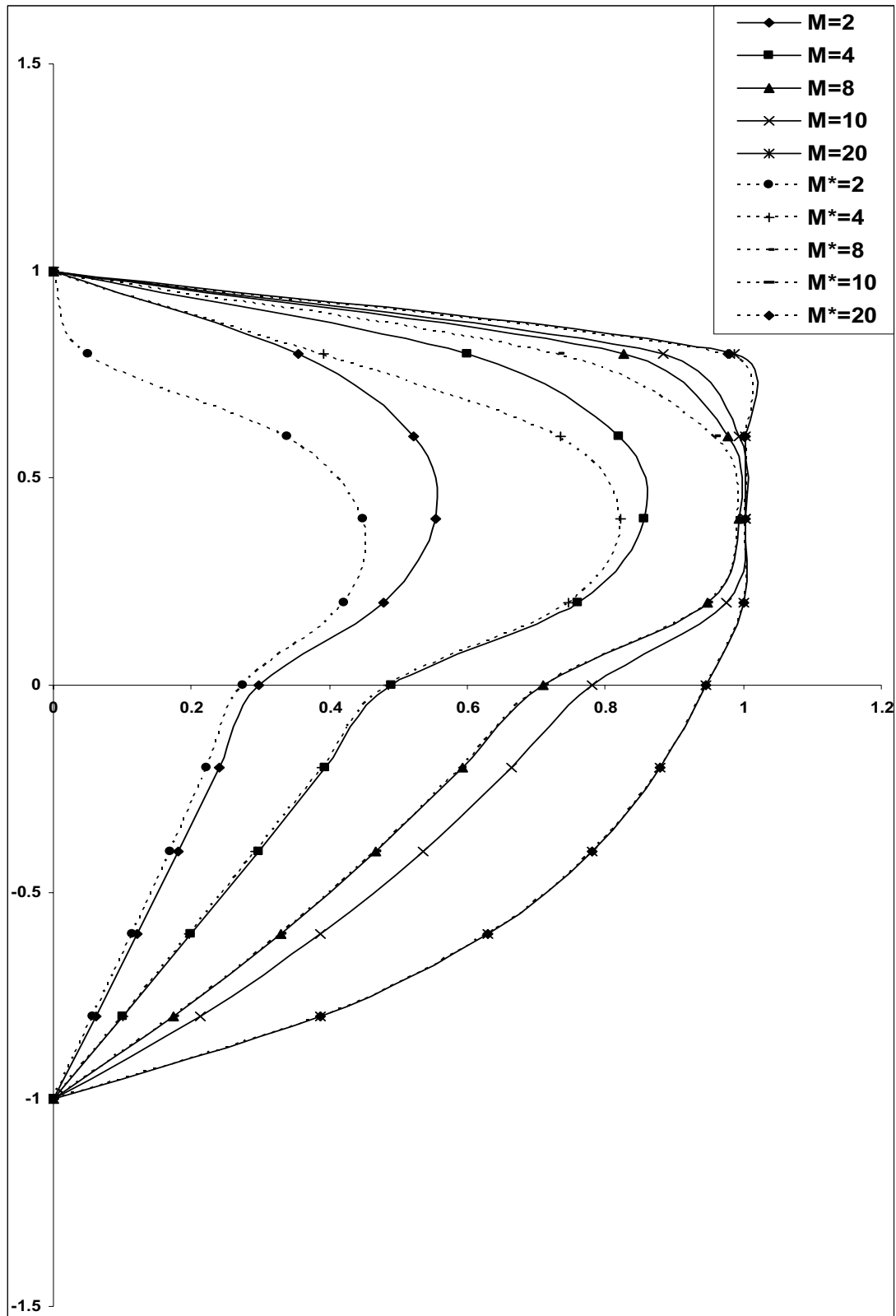


Fig.2. Velocity profiles  $u_1, u_2$  (unsteady flow),  $u_1^*, u_2^*$  (steady flow) for different  $M$  and  $\alpha = 0.333, \sigma = 0.1, h = 0.75, R_e = -1, \lambda = 0.8, \varepsilon = 0.5, \omega = 1, t = \pi / \omega$ .

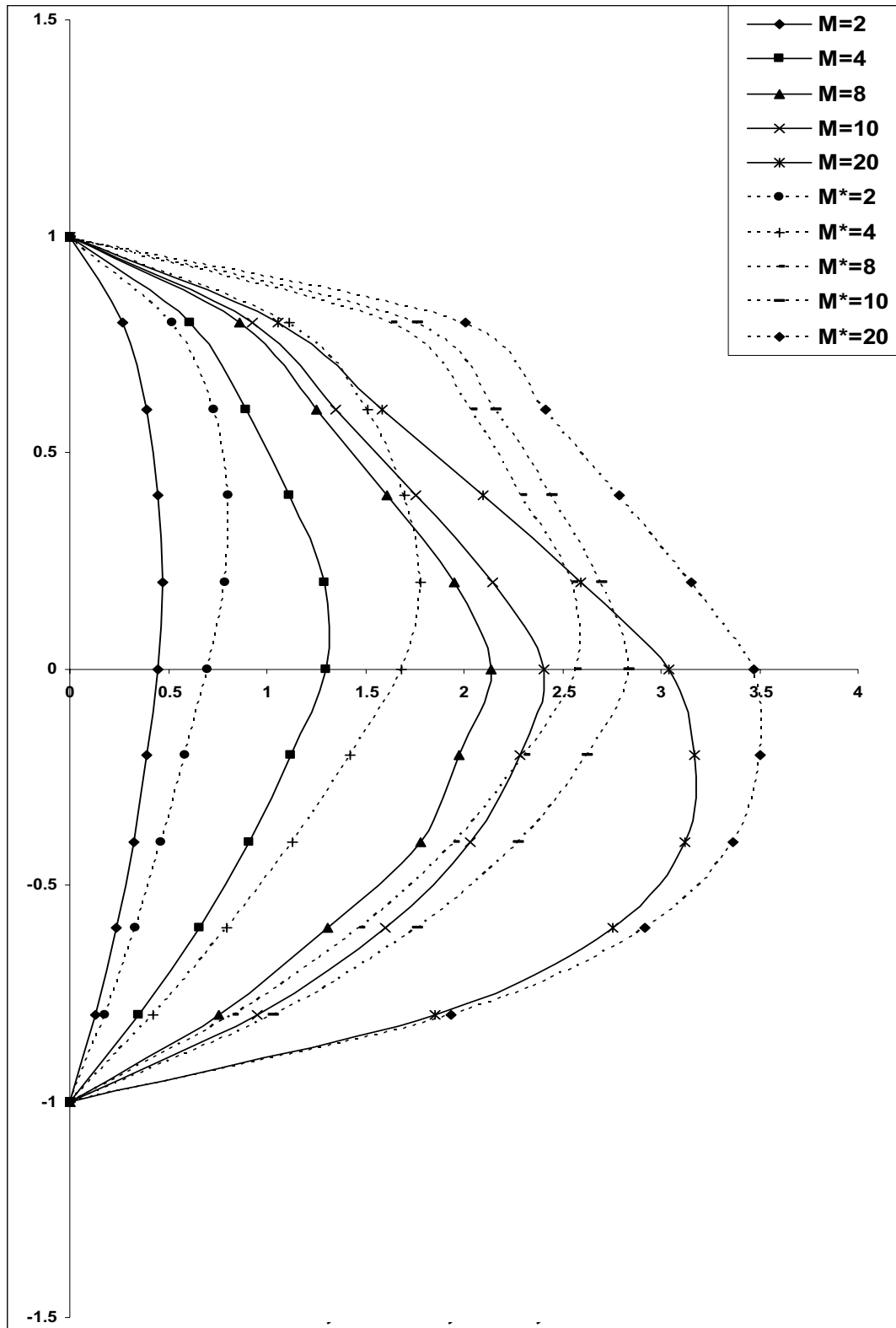


Fig.3. Temperature profiles  $\theta_1, \theta_2$  (unsteady flow),  $\theta_1^*, \theta_2^*$  (steady flow) for different  $M$  and  $\beta = 1, \alpha = 0.333, \sigma = 0.1, h = 0.75, R_e = -1, \lambda = 0.2, \varepsilon = 0.5, \omega = 1, t = \pi / \omega$ .

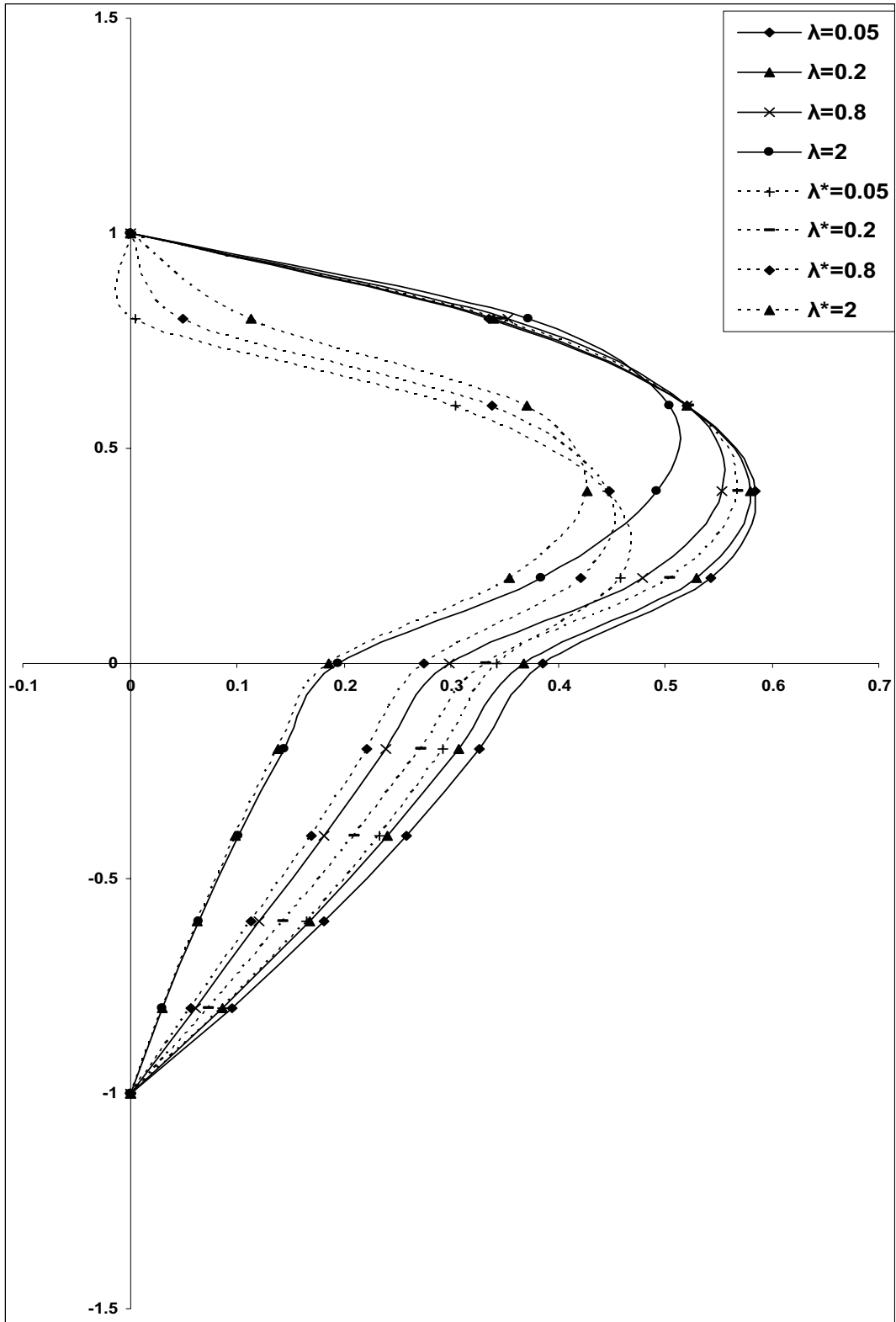


Fig.4. Velocity profiles  $u_1, u_2$  (unsteady flow),  $u_1^*, u_2^*$  (steady flow) for different  $\lambda$  and  $M=2$ ,  $\alpha = 0.333, \sigma = 0.1, R_e = -1, h = 0.75, \varepsilon = 0.5, \omega = 1, t = \pi / \omega$ .

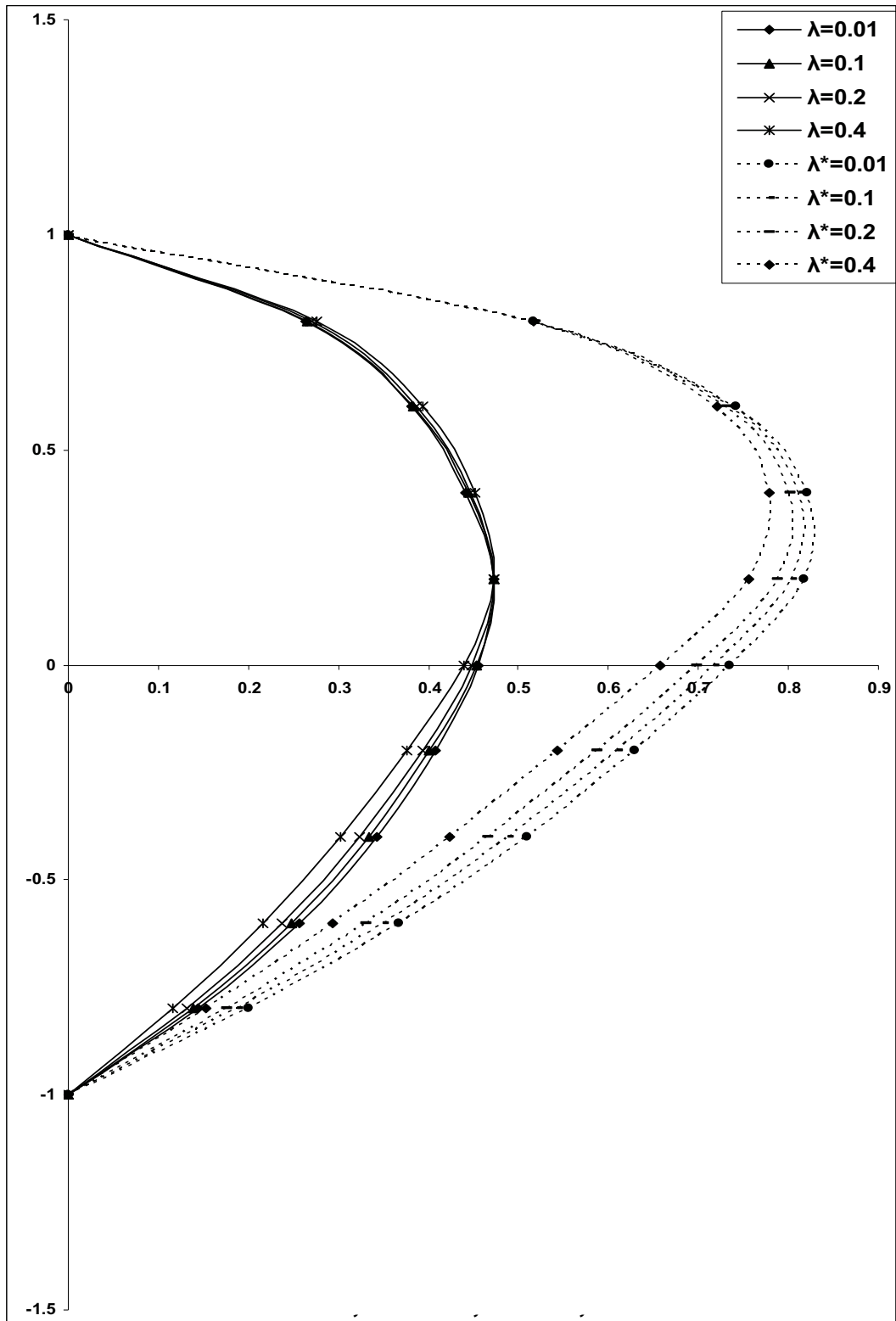


Fig.5. Temperature profiles  $\theta_1, \theta_2$  (unsteady flow),  $\theta_1^*, \theta_2^*$  (steady flow) for different  $\lambda$  and  $\beta=1, M=2, \alpha=0.333, \sigma=0.1, R_e=-1, h=0.75, \varepsilon=0.5, \omega=1, t=\pi/\omega$ .

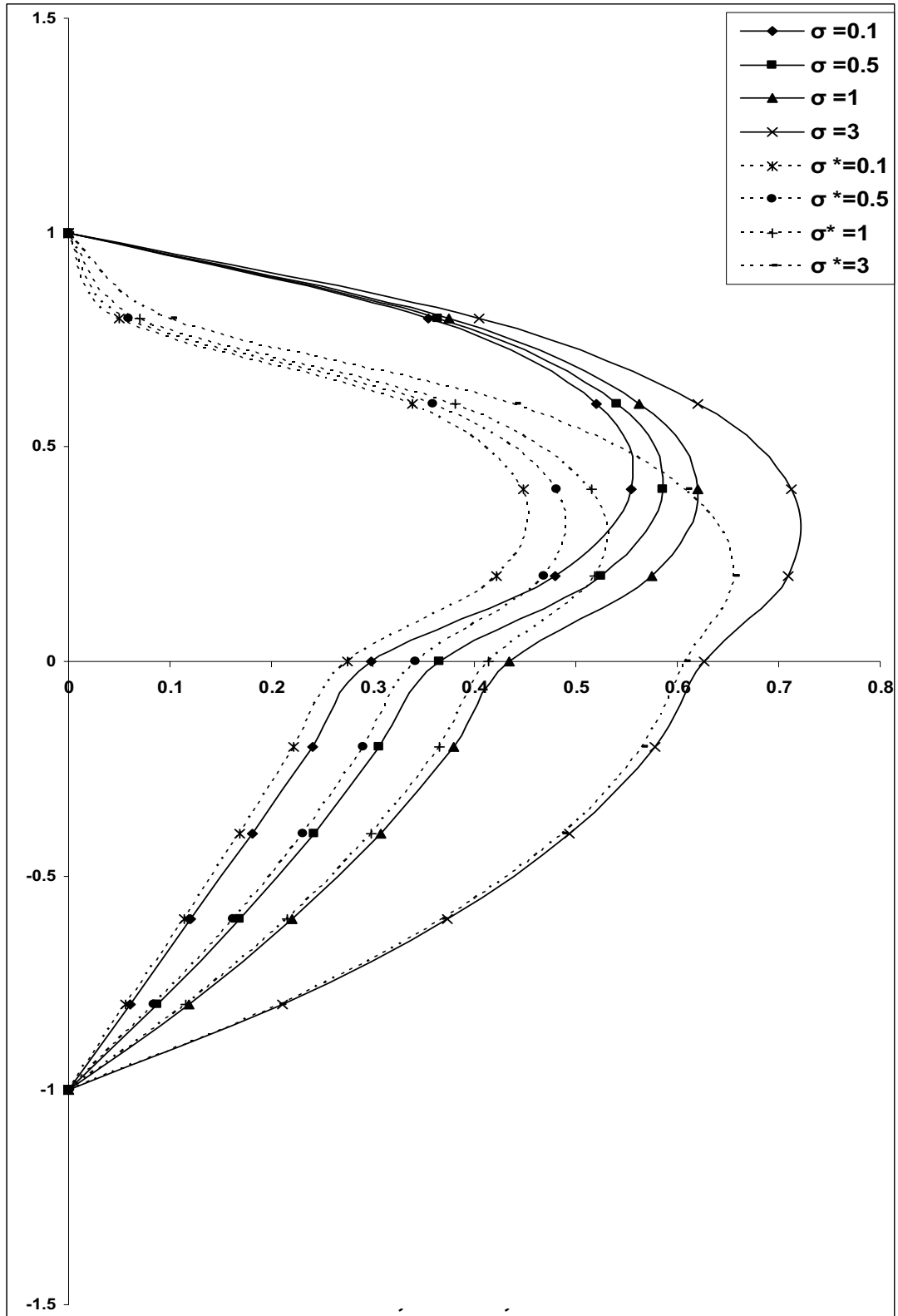


Fig.6. Velocity profiles  $u_1, u_2$  (unsteady flow),  $u_1^*, u_2^*$  (steady flow) for different  $\sigma$  and  $M=2$   
 $\alpha = 0.333, h = 0.75, R_e = -1, \lambda = 0.8, \varepsilon = 0.5, \omega = 1, t = \pi / \omega$ .

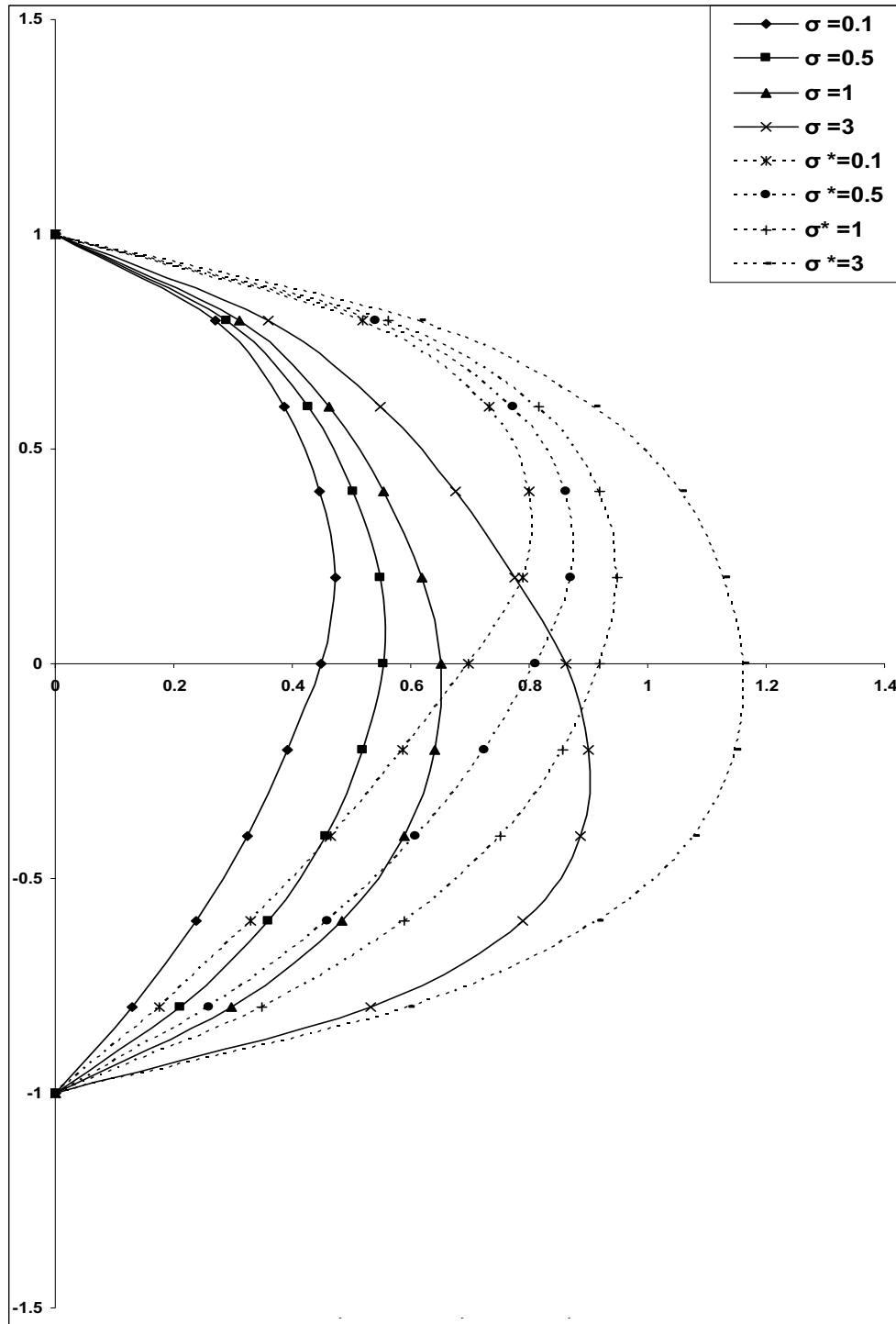


Fig.7. Temperature profiles  $\theta_1, \theta_2$  (unsteady flow),  $\theta_1^*, \theta_2^*$  (steady flow) for different  $\sigma$  and  $\beta = 1, M = 2, \alpha = 0.333, h = 0.75, R_e = -1, \lambda = 0.2, \varepsilon = 0.5, \omega = 1, t = \pi / \omega$ .

The effect of the ratio of viscosities  $\alpha$  on velocity and temperature distributions of the two fluids is shown in Figs 8 and 9, respectively. From Fig.8, it is observed that an increase in  $\alpha$  increases the velocity distributions in the two fluid regions. But from Fig.9, the temperature distributions  $\theta_1$  and  $\theta_2$  are found to decrease as  $\alpha$  increases. The maximum velocity distribution in the channel tends to move above the channel

centre line towards region-I as  $\alpha$  increases, while the temperature distribution in the channel tends to move slightly above the channel centre line towards region-I.

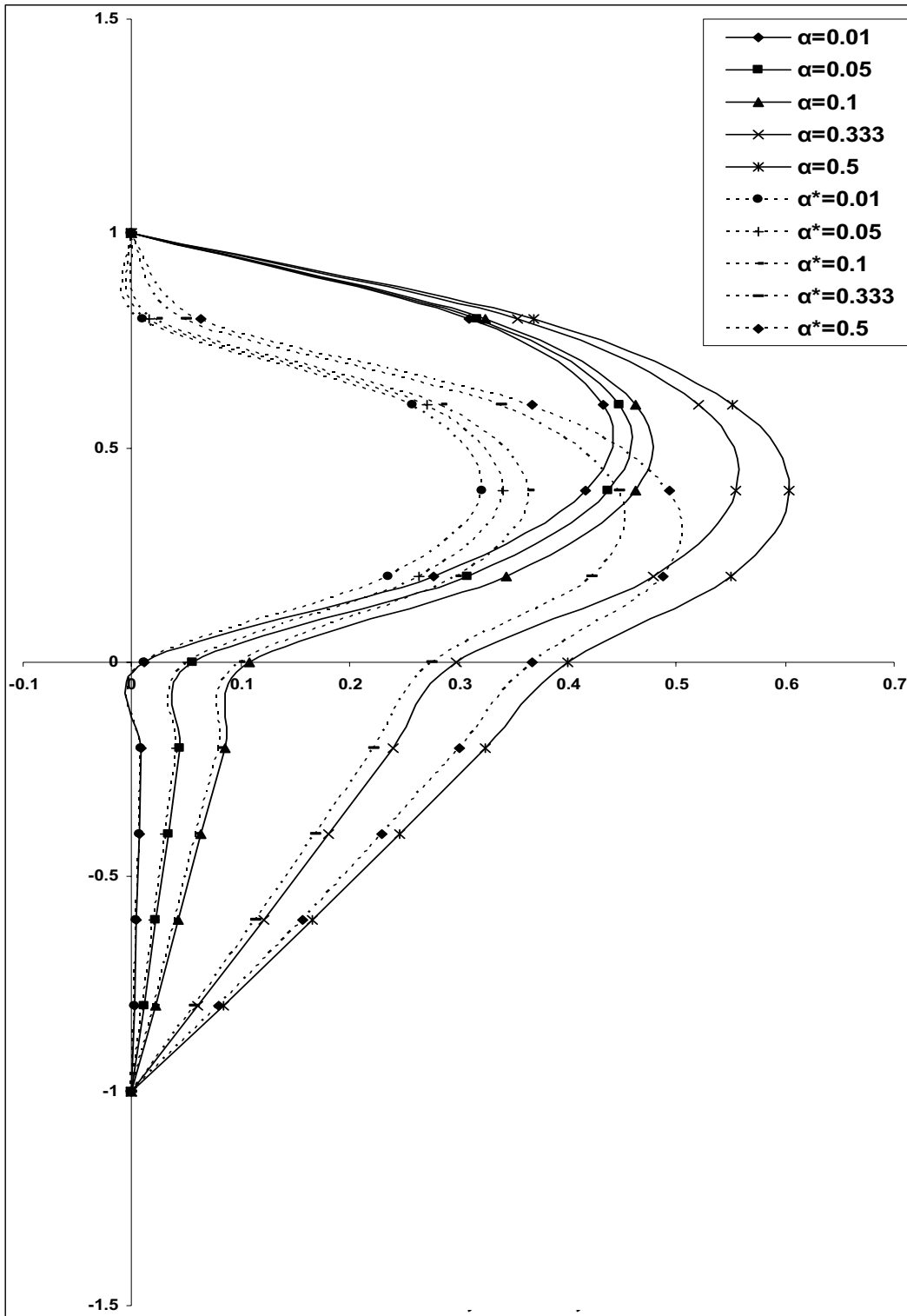


Fig.8. Temperature profiles  $\theta_1, \theta_2$  (unsteady flow),  $\theta_1^*, \theta_2^*$  (steady flow) for different  $\alpha$  and  $M = 2, \sigma = 0.1, h = 0.75, R_e = -1, \lambda = 0.8, \varepsilon = 0.5, \omega = 1, t = \pi / \omega$ .



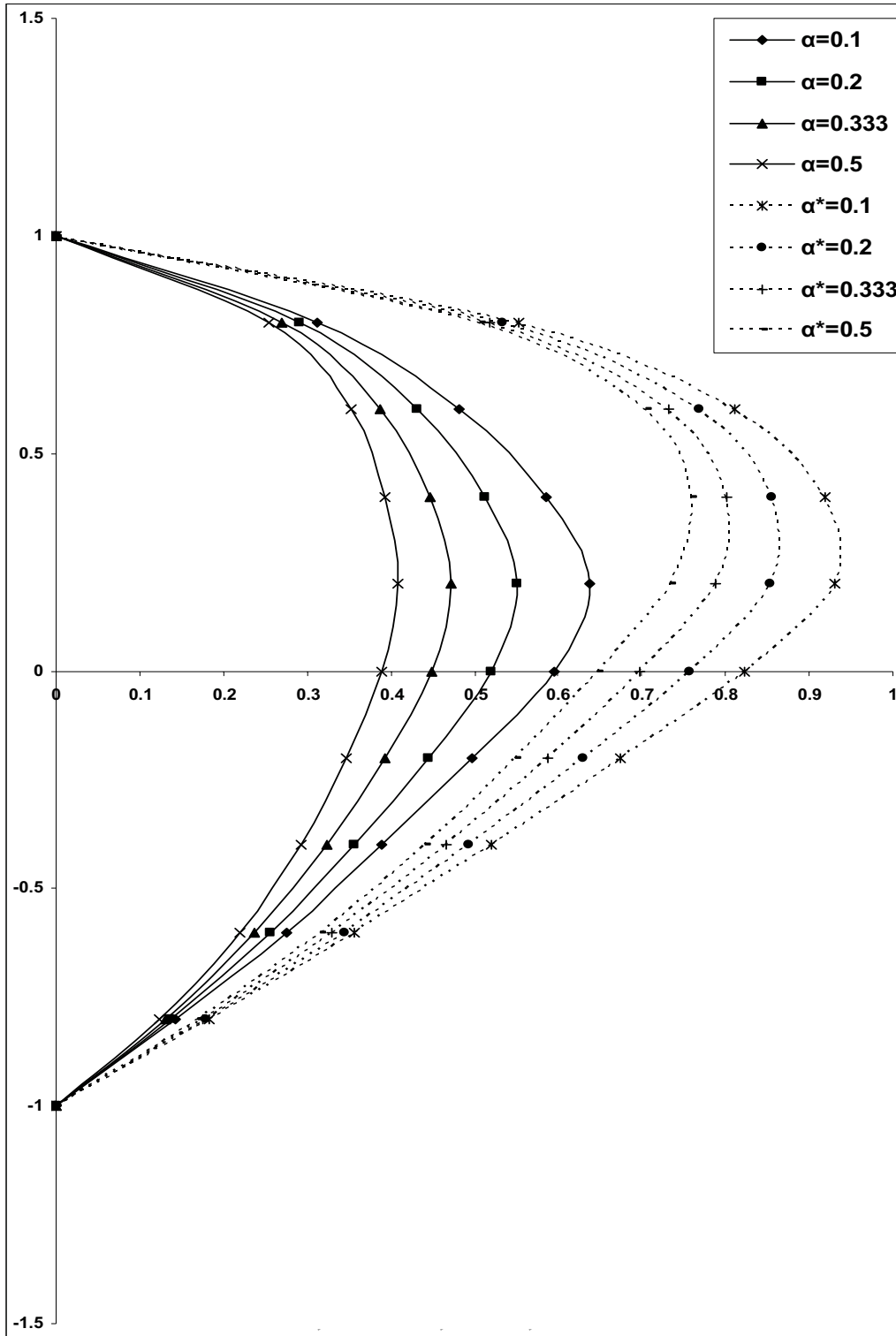


Fig.9. Temperature profiles  $\theta_1, \theta_2$  (unsteady flow),  $\theta_1^*, \theta_2^*$  (steady flow) for different  $\alpha$  and  $\beta = 1, M=2, \sigma = 0.1, h = 0.75, R_e = -1, \lambda = 0.2, \varepsilon = 0.5, \omega = 1, t = \pi / \omega$ .

The effect of varying the height ratio  $h$  on velocity and temperature distributions is shown in Figs 10 and 11, respectively. It is found that an increasing  $h$  increases the velocity and temperature distributions in

the two regions. Also, the maximum velocity and temperatures in the channel tend to move above the channel centre line towards region-I as  $h$  increases.

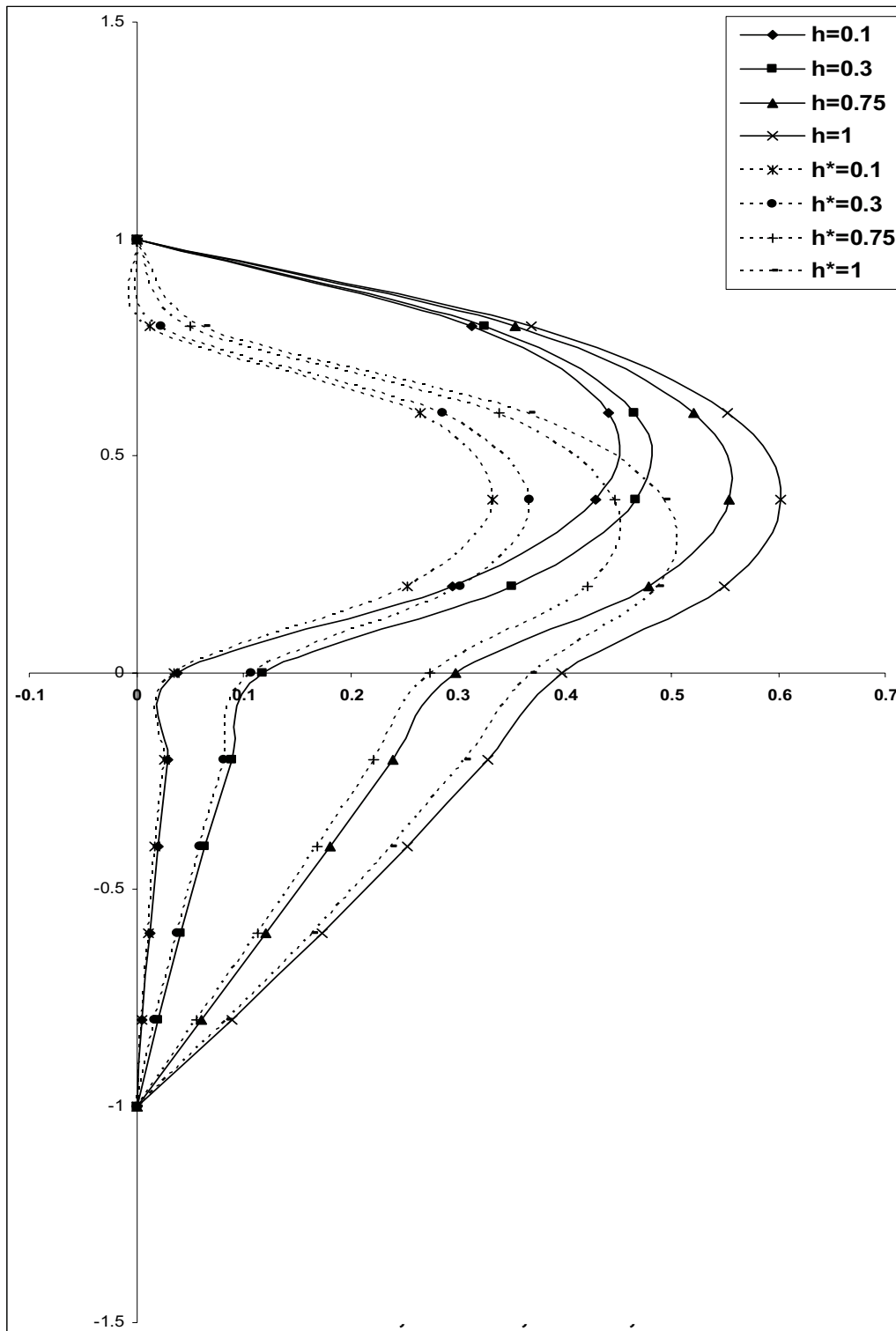


Fig.10. Velocity profiles  $u_1, u_2$  (unsteady flow),  $u_1^*, u_2^*$  (steady flow) for different  $h$  and  $M = 2, \alpha = 0.333, \sigma = 0.1, R_e = -1, \lambda = 0.8, \varepsilon = 0.5, \omega = 1, t = \pi / \omega$ .

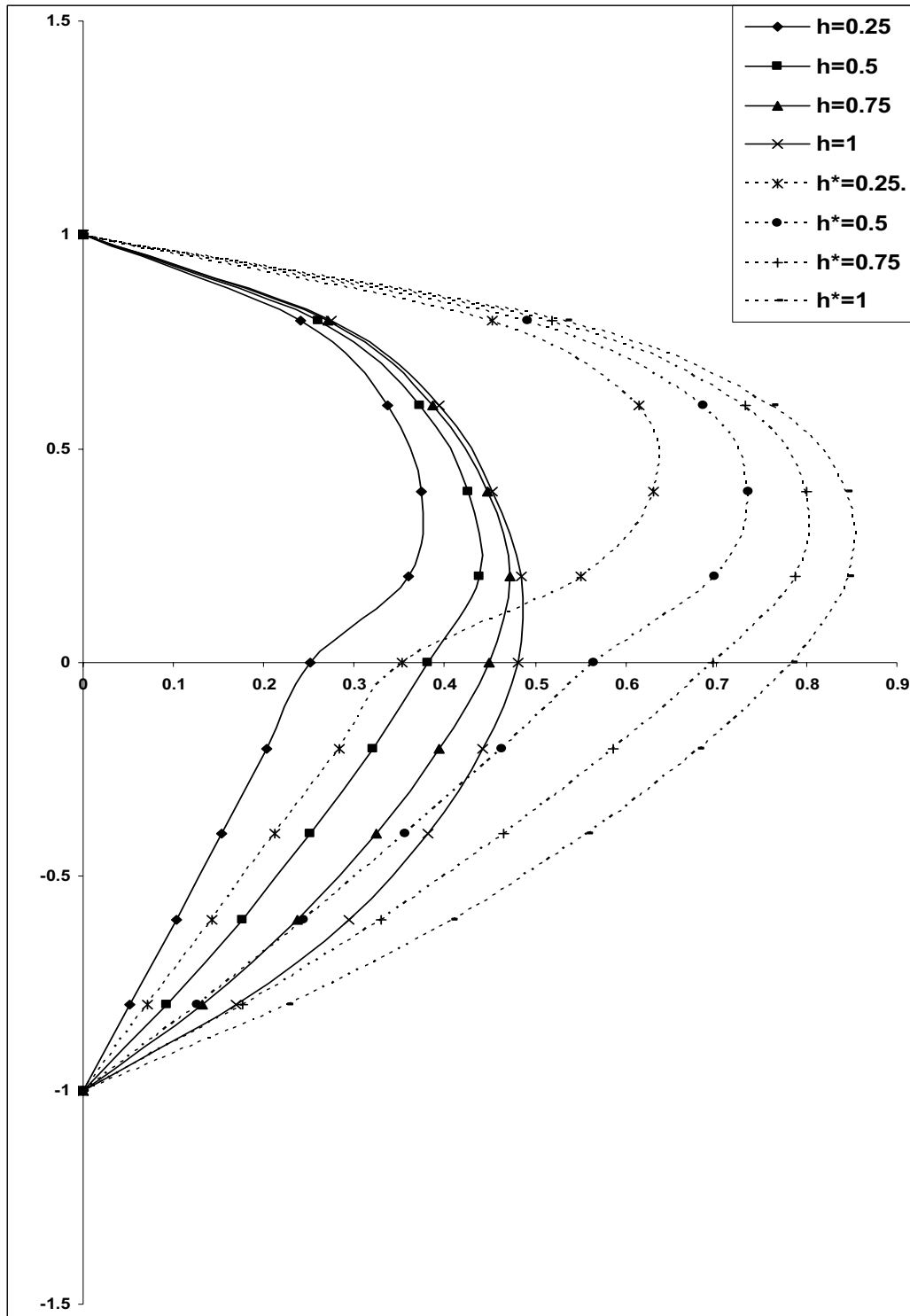


Fig.11. Temperature profiles  $\theta_1, \theta_2$  (unsteady flow),  $\theta_1^*, \theta_2^*$  (steady flow) for different  $h$  and  $\beta = 1$ ,  $M=2$ ,  $\alpha = 0.333, \sigma = 0.1, R_c = -1, \lambda = 0.2, \varepsilon = 0.5, \omega = 1, t = \pi / \omega$ .

The effect of the thermal conductivity ratio  $\beta$  on the temperature distribution is shown in Fig.12. It is observed that an increasing  $\beta$  increases the temperature distribution in both fluid regions. Also, the maximum temperature in the channel tends to move above the channel centre line towards region-I as  $\beta$  increases.

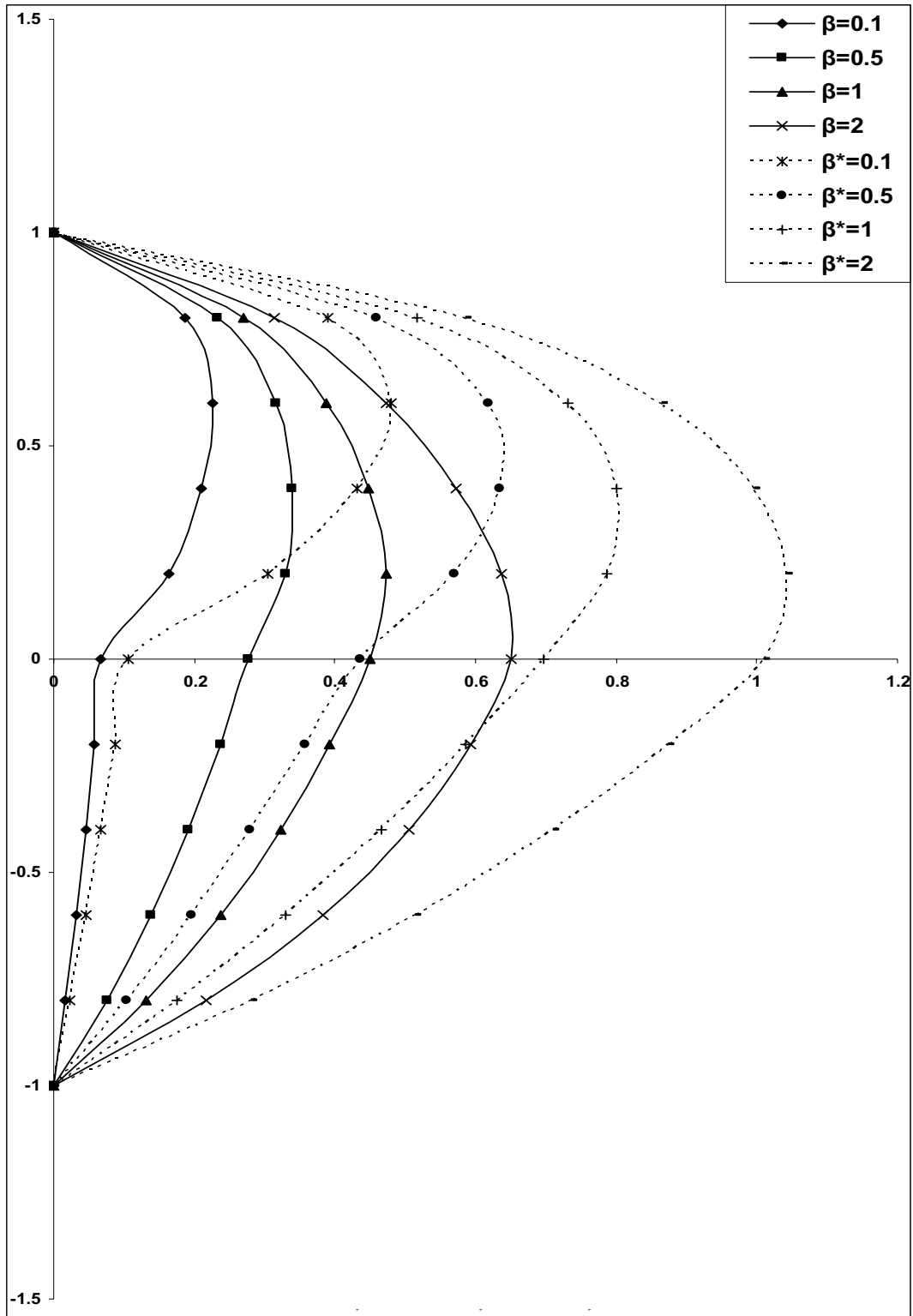


Fig.12. Temperature profiles  $\theta_1, \theta_2$  (unsteady flow),  $\theta_1^*, \theta_2^*$  (steady flow) for different  $\beta$  and  $\lambda = 0.2, M=2, \alpha = 0.333, \sigma = 0.1, R_e = -1, h = 0.75, \varepsilon = 0.5, \omega = 1, t = \pi / \omega$ .

## 5. Conclusions

The governing equations for an unsteady MHD two-fluid flow and heat transfer of an electrically conducting fluids through a horizontal channel bounded by two parallel porous plates (in which one is stationary and the other oscillating) under the influence of an applied transverse magnetic field are formulated, assuming that the two-fluids are of different viscosities, electrical and thermal conductivities. The resulting partial differential equations are transformed in to a set of ordinary linear differential equations using two-term series as a combination of both steady state and transient time dependent parts and are solved in closed form. Numerical calculations of these solutions are performed and these are represented graphically to discuss the behaviour of the flow and heat transfer and their dependence on some of the physical parameters involved in the study, such as the Hartmann number  $M$ , porous parameter  $\lambda$ ; the ratios of viscosities  $\alpha$ , heights  $h$ , electrical and thermal conductivities:  $\sigma$  and  $\beta$  respectively. It is found that when the strength of the magnetic field is increased, the velocity and temperature are enhanced and hence the fluid velocity increased. Also, the maximum velocity in the channel tends to move above the channel centre line towards region-I (i.e., upper fluid region) as the strength of the magnetic field is increased, when all the remaining governing parameters are fixed. The velocity distributions in the two regions increase as  $\lambda$  increases. The maximum velocity distribution in the channel tends to move above the channel center line towards region-I as  $\lambda$  increases. It is observed that the temperature increases in the upper region and decreases in the lower as  $\lambda$  increases. And it is found that the effect of increasing the thermal conductivity ratio increases the temperature distributions in both the regions. Also, the maximum temperature in the channel tends to move above the channel centre line towards region-I (i.e., for the fluid in the upper region). Finally it is concluded that the velocity distributions in the two regions are pronounced more in the unsteady state when compared to the steady case, but the temperature distributions in the two regions is pronounced more in the steady state case than in the unsteady state case.

Finally, it is concluded that with the suitable values of ratios of the Hartmann number, porous parameter, electrical and thermal conductivities, also heights, the velocity and temperature can be increased. Although the validity of the obtained results is not verified practically, the fact is that the solutions satisfy all boundary and interface conditions (as shown in the profiles) and hence there is some conformity with the theoretical results are concerned.

## Nomenclature

- $a_1, b_1, c_1$  – functions/real constants represented in the solutions  
 $d_1, m_1$   
 $B_0$  – applied uniform transverse magnetic field  
 $E_0$  – constant electric field in the  $z$ -direction  
 $h$  – ratio of the heights of the two regions  
 $h_1$  – height of the channel in the upper region  
 $h_2$  – height of the channel in the lower region  
 $K_1, K_2$  – thermal conductivities of the two fluids  
 $M$  – Hartmann number  
 $P$  – pressure  
 $R_e$  – electric load parameter  
 $T_1, T_2$  – temperatures of the fluids in the two regions respectively  
 $T_{w_1}, T_{w_2}$  – constant temperatures at both the walls  
 $t$  – time  
 $u_p = \left( -\frac{\partial p}{\partial x} \right) \frac{h_1^2}{\mu_1}$ , the characteristic velocity  
 $u_1, u_2$  –  $x$ - component of velocity distributions in the two fluid regions

- $u_{01}(y)$  – velocity distributions in the basic steady state case in two regions  
 $u_{02}(y)$   
 $u_{11}(y)$  – time dependent velocity components  
 $u_{12}(y)$   
 $(x, y, z)$  – space co-ordinates  
 $\alpha$  – ratio of the viscosities  
 $\beta$  – ratio of thermal conductivities  
 $\varepsilon$  – amplitude (a small constant quantity such that  $\varepsilon \ll 1$ )  
 $\theta_1, \theta_2$  – non-dimensional forms of temperature distributions of the two fluids  
 $\theta_{01}(y)$  – temperature distributions in the basic steady state case in two regions  
 $\theta_{02}(y)$   
 $\theta_{11}(y)$  – time dependent components of the temperatures in the two regions  
 $\theta_{12}(y)$   
 $\lambda$  – porous parameter  
 $\mu_1, \mu_2$  – viscosities of the two fluids  
 $\rho$  – density  
 $\sigma$  – ratio of electrical conductivities  
 $\sigma_1, \sigma_2$  – electrical conductivities of the two fluids  
 $\omega$  – frequency of oscillation

### Subscripts

1,2 – refers to the quantities in the upper and lower fluid regions respectively

### References

- Chamkha A.J. (2000): *Flow of two-immiscible fluids in porous and non-porous channels*. – ASME J. Fluids Engineering, vol.122, pp.117-124.  
 Chamkha A.J. (2004): *Unsteady MHD convective heat and mass transfer past a semi-infinite vertical permeable moving plate with heat absorption*. – Int. J. Eng. Sci., vol.42, pp.217-230.  
 Chan C.K. (1979): *Finite element formulation and solution of nonlinear heat transfer*. – J. Nuclear Engg., and Design, vol.51, p.253.  
 Chandran N.P., Nirmal C. Sacheti and Ashok K. Singh (1998): *Unsteady hydromagnetic free convection flow with heat flux and accelerated boundary motion*. – J. Phys. Soc. Japan, vol.67, No.1, pp.124-129.  
 Chao J., Mikic B.B. and Todreas N.E. (1979): *Radiation streaming in power reactors: proceedings of the special session American Nuclear Society (ANS) Winter Meeting, Washington, D.C.* – Nuclear Technology, vol.42. p.22.  
 Dunn P.F. (1980): *Single-phase and two-phase magnetohydrodynamic pipe flow*. – Int. J. Heat Mass Transfer, vol.23, p.373.  
 Gherson P. and Lykoudis P.S. (1984): *Local measurements in two-phase liquid-metal magneto-fluid mechanic flow*. – J. Fluid Mechanics, vol.147, pp.81-104.  
 Griffith P. and Wallis G.B. (1961): *Two-phase slug flow*. – Heat Transfer, Transactions of ASME, 83C, pp.307-320.  
 Gupta A.S. (1960): *On the flow an electrically conducting fluid near an accelerated plate in the presence of a magnetic field*. – J. Phys. Soc. Japan, vol.15, No.10, pp.1894-1897.  
 Haim H.B., Jianzhong Z., Shizhi Q. and Yu X. (2003): *A magneto-hydrodynamically controlled fluidic network*. – Sensors and Actuators B, vol.88, No.2, pp.205–216.

- Hussameddine S.K., Martin J.M. and Sang W.J. (2008): *Analytical prediction of flow field in magnetohydrodynamic-based microfluidic devices*. – Journal of Fluids Engineering, vol.130, No.9, p.6.
- Katagiri M. (1962): *Flow formation in Couette motion in magnetohydrodynamics*. – J. Phys. Soc. Japan, vol.17, No.2, pp.393-396.
- Lielausis O. (1975): *Liquid metal magnetohydrodynamics*. – Atom. Energy Rev., vol.13, p.527.
- Linga Raju T. and Murty P.S.R. (2005): *Quasi-steady state solutions of MHD ionized flow and heat transfer with hall currents between parallel walls in a rotating system*. – Bulletin of Pure and Applied Sciences (An International Research Journal of Sciences), Section-E, Maths. & Stat. Delhi, India, vol.24E, No.2, pp.467-490.
- Linga Raju T. and Murty P.S.R. (2006): *Hydromagnetic two-phase flow and heat transfer through two parallel plates in a rotating system*. – J. Indian Academy of Mathematics, Indore, India, vol.28, No.2, pp.343-360.
- Linga Raju T. and Sreedhar S. (2009): *Usteady two-fluid flow and heat transfer of conducting fluids in channels under transverse magnetic field*. – Int. J. of Applied Mechanics and Engineering, vol.14, No.4, pp.1093-1114.
- Lohrasbi J. and Sahai V. (1989): *Magnetohydrodynamic heat transfer in two-phase flow between parallel plates*. – Applied Scientific Research, vol.45, pp.53-66.
- Malashetty M.S. and Leela V. (1992): *Magnetohydrodynamic heat transfer in two phase flow*. – Int. J. Engng. Sci., vol.30, pp.371-377.
- Michiyoshi Funakawa Kuramoto C., Akita Y. and Takahashi O. (1977): *Instead of the helium-lithium annular-mist flow at high temperature, an air-mercury stratified flow in a horizontal rectangular duct in a vertical magnetic field* – Int. J. Multiphase Flow, vol.3, p.445.
- Muhuri P.K. (1963): *Flow formation in couette motion in magnetohydrodynamics in the suction*. – J. Phys. Soc. Japan, vol.18, No.11, pp.1671.
- Pakham B.A. and Shail R. (1971): *Stratified laminar flow of two immiscible fluids*. – Proceedings of the Cambridge Philosophical Society, vol.69, pp.443-448.
- Pallath C., Nirmal C. Sacheti and Ashok K. Singh (1998): *Unsteady hydromagnetic free convection flow with heat flux and accelerated boundary motion*. – J. of the Physical Soc. of Japan, vol.67, p.124.
- Pop I. (1968): *On the hydromagnetic flow near an accelerated plate*. – Zeitschrift fur Angewandte Mathematik and Mechanik (ZAMM), vol.48, pp.69-70.
- Ramadan H.M. and Chamkha A.J. (1999): *Two-phase free convection flow over an infinite permeable inclined plate with non-uniform particle-phase density*. – Int. J. Engng. Sci., vol.37, p.1351.
- Schlichting H. (1955): *Boundary Layer Theory*. – New York: McGraw Hill Book Company, Inc., pp.66.
- Serizawa A., Ida T., Takahashi O. and Michiyoshi I. (1990): *MHD effect on Nak-nitrogen two-phase flow and heat transfer in a vertical round tube*. – Int. J. Multi-Phase Flow, vol.16(5), p.761.
- Shail R. (1973): *On laminar two-phase flow in magneticohydrodynamics*. – Int. J. Engng. Sci., vol.11, pp.1103-1108.
- Shipley D.G. (1984): *Two-phase flow in large diameter pipes*. – Chemical Engineering Science, vol.39, pp.163-165.
- Soundalgekar M. (1967): *On the flow of an electrically conducting incompressible fluid near an accelerated plate in the presence of a parallel plate, under transverse magnetic field*. – Proc. Indian Academy of Science, vol.A65, pp.179-187.
- Stanisic M.M., Fetz B.H., Mickelsen Jr. H.P. and Czumak F.M. (1962): *On the flow of a hydromagnetic fluid between two oscillating flat plates*. – Journal of Aero/Space Science, vol.29, No.1, p.116-117.
- Tao L.N. (1960): *Magnetohydrodynamic effects on the formation of Couette flow*. – Journal of Aero/Space Science, vol.27, pp.334-338.
- Tsuyoshi I. and Shu-Ichiro I. (2008): *Two-fluid magnetohydrodynamic simulation of converging hi flows in the interstellar medium*. – The Astrophysical Journal, vol.687, No.1, pp.303-310.
- Umavathi J.C., Abdul Mateen, Chamkha A.J. and Al-Mudhaf A. (2006): *Oscillatory Hartmann two-fluid flow and heat transfer in a horizontal channel*. – Int. J. of Applied Mechanics and Engineering, vol.11, No.1, pp.155-178.

- Varma P.D. and Gaur Y.N. (1972): *unsteady flow and temperature distribution of a viscous incompressible fluid between two parallel plate plates.* – Proc. Indian Acad. Sci., vol.75, pp.108.
- Weston M.C., Gerner M.D., and Fritsch I. (2010): *Magnetic fields for fluid motion.* – Analytical Chemistry, vol.82, No.9, pp.3411-3418.
- Yi M., Qian S. and Bau H. (2002): *A magnetohydrodynamic chaotic stirrer.* – Journal of Fluid Mechanics, vol.468, pp.153–177.

## Appendix

$$\begin{aligned}
 a_1 &= M^2, & a_2 &= M^2 R_e - 1, & a_3 &= \varepsilon \cos \omega t, & a_4 &= \lambda a_3, \\
 a_5 &= -\varepsilon \sin \omega t + M^2 a_3, & a_6 &= \frac{a_4}{a_3}, & a_7 &= \frac{a_5}{a_3}, & a_8 &= M^2 h^2 \alpha \sigma, \\
 a_9 &= M^2 h^2 \alpha \sigma R_e - \alpha h^2, & a_{10} &= \lambda a_3, & a_{11} &= -\varepsilon \omega \sin \omega t + M^2 h^2 \alpha \sigma a_3, \\
 a_{12} &= \frac{a_{10}}{a_3}, & a_{13} &= \frac{a_{11}}{a_3}, & a_{14} &= m_2 - m_1, & a_{15} &= \frac{a_2}{a_1} e^{-m_1}, \\
 a_{16} &= -m_4 + m_3, & a_{17} &= \frac{a_9}{a_8} e^{m_3}, & a_{18} &= 1 - e^{a_{14}}, & a_{19} &= 1 - e^{a_{16}}, \\
 a_{20} &= a_{17} - \frac{a_9}{a_8} - a_{15} + \frac{a_2}{a_1}, & a_{21} &= m_2 - m_1 e^{a_{14}}, \\
 a_{22} &= \frac{m_4 - m_3 e^{a_{16}}}{\alpha h}, & a_{23} &= \frac{a_{17} m_3}{\alpha h} - a_{15} m_1, \\
 a_{24} &= a_{18} a_{22} - a_{21} a_{19}, & a_{25} &= a_{20} a_{22} - a_{23} a_{19}, \\
 a_{26} &= \frac{a_{25}}{a_{24}}, & a_{27} &= \frac{-a_{23} + a_{26} a_{21}}{a_{22}}, & a_{28} &= m_6 - m_5, \\
 a_{29} &= -m_8 + m_7, & a_{30} &= 1 - e^{a_{28}}, & a_{31} &= 1 - e^{a_{29}}, \\
 a_{32} &= -e^{-m_5}, & a_{33} &= m_6 - m_5 e^{a_{28}}, & a_{34} &= \frac{m_8 - m_7 e^{a_{29}}}{\alpha h}, \\
 a_{35} &= -m_5 e^{-m_5}, & a_{36} &= a_{30} a_{34} - a_{33} a_{31}, & a_{37} &= a_{32} a_{34} - a_{35} a_{31}, \\
 a_{38} &= \frac{a_{37}}{a_{36}}, & a_{39} &= \frac{-a_{35} + a_{38} a_{33}}{a_{34}}, \\
 b_1 &= m_1^2 c_1^2, & b_2 &= m_2^2 c_2^2, & b_3 &= 2m_1 m_2 c_1 c_2,
 \end{aligned}$$



$$\begin{aligned}
b_4 &= m_1 + m_2, & b_5 &= M^2 c_1^2, & b_6 &= M^2 c_2^2, \\
b_7 &= M^2 \left( \frac{a_2}{a_1} \right)^2, & b_8 &= 2M^2 c_1 c_2, & b_9 &= 2M^2 c_2 \frac{a_2}{a_1}, \\
b_{10} &= 2M^2 c_1 \frac{a_2}{a_1}, & b_{11} &= 2M^2 c_1 R_e, \\
b_{12} &= 2M^2 c_2 R_e, & b_{13} &= 2M^2 R_e \frac{a_2}{a_1} - M^2 R_e^2, & b_{14} &= b_1 + b_5, \\
b_{15} &= b_2 + b_6, & b_{16} &= b_{11} - b_{10}, & b_{17} &= -b_9 + b_{12}, \\
b_{18} &= b_3 + b_8, & b_{19} &= -b_7 + b_{13}, & b_{20} &= \frac{\beta}{\alpha}, & b_{21} &= M^2 h^2 \sigma \beta, \\
b_{22} &= b_{20} m_3^2 c_3^2, & b_{23} &= b_{20} m_4^2 c_4^2, & b_{24} &= 2b_{20} m_3 m_4 c_3 c_4, \\
b_{25} &= m_3 + m_4, & b_{26} &= b_{21} c_3^2, & b_{27} &= b_{21} c_4^2, \\
b_{28} &= b_{21} \left( \frac{a_9}{a_8} \right)^2, & b_{29} &= 2c_3 c_4 b_{21}, & b_{30} &= 2c_4 \frac{a_9}{a_8} b_{21}, \\
b_{31} &= 2c_3 \frac{a_9}{a_8} b_{21}, & b_{32} &= 2b_{21} c_3 R_e, & b_{33} &= 2b_{21} c_4 R_e, \\
b_{34} &= 2b_{21} R_e \frac{a_9}{a_8} - b_{21} R_e^2, & b_{35} &= b_{22} + b_{26}, & b_{36} &= b_{23} + b_{27}, \\
b_{37} &= -b_{31} + b_{32}, & b_{38} &= -b_{30} + b_{33}, & b_{39} &= b_{24} + b_{29}, \\
b_{40} &= -b_{28} + b_{34}, & b_{41} &= -\frac{-b_{14}}{4m_1^2 - 2m_1\lambda}, & b_{42} &= -\frac{-b_{15}}{4m_2^2 - 2m_2\lambda}, \\
b_{43} &= \frac{-b_{16}}{m_1^2 - m_1\lambda}, & b_{44} &= \frac{-b_{17}}{m_2^2 - m_2\lambda}, & b_{45} &= \frac{-b_{18}}{b_4^2 - b_4\lambda}, \\
b_{46} &= -\frac{b_{19}}{\lambda}, & b_{47} &= -\frac{-b_{35}}{4m_3^2 - 2m_3\lambda}, & b_{48} &= -\frac{-b_{36}}{4m_4^2 - 2m_4\lambda},
\end{aligned}$$

$$\begin{aligned}
b_{49} &= \frac{-b_{37}}{m_3^2 - m_3\lambda}, & b_{50} &= \frac{-b_{38}}{m_4^2 - m_4\lambda}, & b_{51} &= \frac{-b_{39}}{b_{25}^2 - b_{25}\lambda}, \\
b_{52} &= -\frac{b_{40}}{\lambda}, & b_{53} &= b_{41}e^{2m_1} + b_{42}e^{2m_2} + b_{43}e^{m_1} + b_{44}e^{m_2} + b_{45}e^{b_4} + b_{46}, \\
b_{54} &= b_{47}e^{-2m_3} + b_{48}e^{-2m_4} + b_{49}e^{-m_3} + b_{50}e^{-m_4} + b_{51}e^{-b_{25}} - b_{52}, \\
b_{55} &= b_{41} + b_{42} + b_{43} + b_{44} + b_{45}, & b_{56} &= b_{47} + b_{48} + b_{49} + b_{50} + b_{51}, \\
b_{57} &= 2b_{41}m_1 + 2b_{42}m_2 + b_{43}m_1 + b_{44}m_2 + b_4b_{45} + b_{46}, \\
b_{58} &= 2b_{47}m_3 + 2b_{48}m_4 + b_{49}m_3 + b_{50}m_4 + b_{51}b_{25} + b_{52}, \\
b_{59} &= -e^\lambda + 1, & b_{60} &= -e^{-\lambda} + 1, & b_{61} &= -b_{54} + b_{56} + b_{53} - b_{55}, \\
b_{62} &= \frac{b_{58}}{\beta h} - b_{57}, & b_{63} &= \frac{b_{62}}{\lambda}, & b_{64} &= \frac{1}{\beta h}, \\
b_{65} &= -b_{60} + b_{64}b_{59}, & b_{66} &= b_{61} - b_{63}b_{59}, & b_{67} &= \frac{b_{66}}{b_{65}}, \\
b_{68} &= \omega \tan \omega t, & b_{69} &= \varepsilon \cos \omega t \cdot m_5^2 c_5^2, & b_{70} &= \varepsilon \cos \omega t \cdot m_6^2 c_6^2, \\
b_{71} &= 2\varepsilon \cos \omega t \cdot m_5 m_6 c_5 c_6, & b_{72} &= m_5 + m_6, & b_{73} &= M^2 \varepsilon \cos \omega t c_5^2, \\
b_{74} &= M^2 \varepsilon \cos \omega t c_6^2, & b_{75} &= 2M^2 \varepsilon \cos \omega t c_5 c_6, & b_{76} &= 2M^2 R_e c_5, \\
b_{77} &= 2M^2 R_e c_6, & b_{78} &= b_{69} + b_{73}, & b_{79} &= b_{70} + b_{74}, & b_{80} &= b_{71} + b_{75}, \\
b_{81} &= \frac{-b_{78}}{4m_5^2 - 2m_5\lambda + b_{68}}, & b_{82} &= \frac{-b_{79}}{4m_6^2 - 2m_6\lambda + b_{68}}, & b_{83} &= \frac{-b_{76}}{m_5^2 - m_5\lambda + b_{68}}, \\
b_{84} &= \frac{-b_{77}}{m_6^2 - m_6\lambda + b_{68}}, & b_{85} &= \frac{-b_{80}}{b_{72}^2 - \lambda b_{72} + b_{68}}, & b_{86} &= 2b_{81}m_5, \\
b_{87} &= 2b_{82}m_6, & b_{88} &= b_{83}m_5, & b_{89} &= b_{84}m_6, \\
b_{90} &= b_{85}b_{72}, & b_{91} &= b_{20}\varepsilon \cos \omega t, & b_{92} &= b_{21}\varepsilon \cos \omega t, \\
b_{93} &= 2b_{21}R_e, & b_{94} &= b_{91}m_7^2 c_7^2, & b_{95} &= b_{91}m_8^2 c_8^2, \\
b_{96} &= 2b_{91}m_7 m_8 c_7 c_8, & b_{97} &= m_7 + m_8, & b_{98} &= b_{92}c_7^2,
\end{aligned}$$

$$\begin{aligned}
b_{99} &= b_{92}c_8^2, & b_{100} &= 2b_{92}c_7c_8, & b_{101} &= b_{93}c_7, \\
b_{102} &= b_{93}c_8, & b_{103} &= b_{94} + b_{98}, & b_{104} &= b_{95} + b_{99}, \\
b_{105} &= b_{96} + b_{100}, & b_{106} &= \frac{-b_{103}}{4m_7^2 - 2m_7\lambda + b_{68}}, & b_{107} &= \frac{-b_{104}}{4m_8^2 - 2m_8\lambda + b_{68}}, \\
b_{108} &= \frac{-b_{101}}{m_7^2 - m_7\lambda + b_{68}}, & b_{109} &= \frac{-b_{102}}{m_8^2 - m_8\lambda + b_{68}}, & b_{110} &= \frac{-b_{105}}{b_{97}^2 - \lambda b_{97} + b_{68}}, \\
b_{111} &= 2b_{106}m_7, & b_{112} &= 2b_{107}m_8, & b_{113} &= b_{108}m_7, \\
b_{114} &= b_{109}m_8, & b_{115} &= b_{97}b_{110}, & b_{116} &= b_{81}e^{2m_5} + b_{82}e^{2m_6} + b_{83}e^{m_5} + b_{84}e^{m_6} + b_{85}e^{b_{72}}, \\
b_{117} &= b_{106}e^{-2m_7} + b_{107}e^{-2m_8} + b_{108}e^{-m_7} + b_{109}e^{-m_8} + b_{110}e^{-b_{97}}, \\
b_{118} &= b_{81} + b_{82} + b_{83} + b_{84} + b_{85}, & b_{119} &= b_{106} + b_{107} + b_{108} + b_{109} + b_{110}, \\
b_{120} &= b_{86} + b_{87} + b_{88} + b_{89} + b_{90}, & b_{121} &= b_{111} + b_{112} + b_{113} + b_{114} + b_{115}, \\
b_{122} &= m_{10} - m_9, & b_{123} &= b_{116}e^{-m_9}, & b_{124} &= -m_{12} + m_{11}, & b_{125} &= b_{117}e^{m_{11}}, \\
b_{126} &= -e^{b_{122}} + 1, & b_{127} &= -e^{b_{124}} + 1, & b_{128} &= b_{119} - b_{125} + b_{123} - b_{118}, \\
b_{129} &= -m_9e^{b_{122}} + m_{10}, & b_{130} &= -\frac{m_{11}}{\beta h}e^{b_{124}} + \frac{m_{12}}{\beta h}, \\
b_{131} &= -\frac{m_{11}}{\beta h}b_{125} + \frac{b_{121}}{\beta h} + m_9b_{123} - b_{120}, & b_{132} &= -b_{127}b_{129} + b_{130}b_{126}, \\
b_{133} &= b_{128}b_{129} - b_{131}b_{126}, & b_{134} &= \frac{b_{133}}{b_{132}}, \\
c_1 &= a_{15} - a_{26}e^{a_{14}}, & c_2 &= a_{26}, & c_3 &= a_{17} - a_{27}e^{a_{16}}, & c_4 &= a_{27}, \\
c_5 &= e^{-m_5} - a_{38}e^{a_{28}}, & c_6 &= a_{38}, & c_7 &= -a_{39}e^{a_{29}}, & c_8 &= a_{39}, \\
d_1 &= -d_2e^\lambda - b_{53}, & d_2 &= b_{63} + b_{67}b_{64}, & d_3 &= -d_4e^{-\lambda} - b_{54}, \\
d_4 &= b_{67}, & d_5 &= -d_6e^{b_{122}} - b_{123}, & d_6 &= \frac{b_{131} + b_{134}b_{130}}{b_{129}},
\end{aligned}$$

$$d_7 = -d_8 e^{b_{124}} - b_{125},$$

$$d_8 = b_{134},$$

$$m_1 = \frac{\lambda + \sqrt{\lambda^2 + 4a_1}}{2},$$

$$m_2 = \frac{\lambda - \sqrt{\lambda^2 + 4a_1}}{2},$$

$$m_3 = \frac{\lambda + \sqrt{\lambda^2 + 4a_8}}{2},$$

$$m_4 = \frac{\lambda - \sqrt{\lambda^2 + 4a_8}}{2},$$

$$m_5 = \frac{a_6 + \sqrt{a_6^2 + 4a_7}}{2},$$

$$m_6 = \frac{a_6 - \sqrt{a_6^2 + 4a_7}}{2},$$

$$m_7 = \frac{a_{12} + \sqrt{a_{12}^2 + 4a_{13}}}{2},$$

$$m_8 = \frac{a_{12} - \sqrt{a_{12}^2 + 4a_{13}}}{2},$$

$$m_9 = \frac{\lambda + \sqrt{\lambda^2 - 4b_{68}}}{2},$$

$$m_{10} = \frac{\lambda - \sqrt{\lambda^2 - 4b_{68}}}{2},$$

$$m_{11} = \frac{\lambda + \sqrt{\lambda^2 - 4b_{68}}}{2},$$

$$m_{12} = \frac{\lambda - \sqrt{\lambda^2 - 4b_{68}}}{2}.$$

Received: March 27, 2012

Revised: May 18, 2013